A novel disulfide-containing monomer for photoinitiator-free self-healable photocured coatings

Progress in Organic Coatings 187 (2024) 108098

Contents lists available at ScienceDirect

Progress in Organic Coatings

journal homepage: www.elsevier.com/locate/porgcoat

A novel disulfide-containing monomer for photoinitiator-free self-healable photocured coatings

Alberto Spessa [a,*], Roberta Bongiovanni [a,b], Alessandra Vitale [a,b,*]

[a] Department of Applied Science and Technology, Politecnico di Torino, Corso Duca degli Abruzzi 24, 10129 Torino, Italy
[b] INSTM – Politecnico di Torino Research Unit, 50121 Firenze, Italy

ARTICLE INFO

Keywords:
Photopolymerization
UV-curable coatings
Disulfide bonds
Self-initiating
Self-healing

ABSTRACT

Disulfide-containing coatings are gaining importance due to the peculiar properties and responsiveness of S—S bonds, which make them suitable for several applications, first among them self-healable materials. Herein, a novel UV-curable diacrylated polyurethane monomer containing disulfide bonds (DSPDA) was synthesized through a one-step process without the need for further purification, as assessed by NMR and HPLC analyses. The photopolymerization kinetics of the monomer was studied through real-time FTIR, highlighting a fast and complete conversion even in the absence of a photoinitiator, thus demonstrating the self-initiating capabilities of the synthesized monomer based on the disulfide cleavage upon UV light exposure. Clear coatings having a T_g = 72 °C were obtained. The self-healing ability of the films was assessed: thanks to the presence of disulfide bonds in the cured coating, a recovery of the damage was obtained in only 10 min by heating at 100 °C.

1. Introduction

Over the past years, photopolymerization has gained significant importance and has become a well-established technique in different fields due to its green and sustainable features [1,2]. In line with the growing attention to environmental protection and energy saving, the use of UV-curable resins has become increasingly popular in various applications, including 3D printing, adhesives, inks, and coatings [3,4]. UV-curable coatings, mainly acrylates and methacrylates, are gradually replacing conventional solvent-based ones, primarily for their low-energy requirements, quick curing process, lack of solvent, and thus decrease in VOC production [5,6]. Photoinitiators are a key component of UV-curable coatings since they are able to produce reactive species after UV light exposure, starting the polymerization reaction [7,8]. In acrylic systems, photoinitiators generate active carbon radicals upon homolytic cleavage or hydrogen abstraction [24], able to attack the acrylic double bonds and initiate the curing process [8,9]. In addition to alkyl radicals, other initiator species have acquired relevance in the field of UV-curing of (meth)acrylates, like phosphinoyl, silyl, thiyl, and many others [3,7]. However, the introduction of a photoinitiator can lead to drawbacks, such as the presence of by-products and migrating species, discoloration, and limited storage stability [10]. Thus, reducing or completely avoiding the use of photoinitiators has several advantages, including cost reduction.

Multiple studies have already focused their attention on photoinitiator-free photocurable systems, in which self-initiating capability is achieved using certain monomers like brominated acrylates [11], diacrylamides [12], or bismaleimides [13]. Moreover, thiol-ene [14,15] and, more recently, disulfide-ene [16,17] chemistries have also been employed in photoinitiator-free formulations. In the case of disulfide-ene, highly reactive thiyl radicals are easily generated by photocleavage of the S—S bond following UV light exposure [18,19]. Until now only a few studies have described the use of disulfide-containing acrylate monomers to obtain a self-initiated UV-curing mechanism [9,20–22].

Several works present in literature have already employed different disulfide-containing monomers as crosslinking agents in UV-curing formulations, to exploit the wide potential of the sulfur-sulfur bond for different applications. In their work, Zhang et al. [9] and Chen et al. [21] introduced 2,2-dithiodiethanol diacrylate into their photoresist formulation to allow degradation of the cured material and a reduction in the volumetric shrinkage during the curing process, respectively. Sáiz et al. [23] used the methacrylated version of the previously described molecule to prolong the service life of a UV-cured coating thanks to disulfide self-healing ability. Furthermore, the use of polyurethane acrylates containing S—S bonds was also reported in formulations for

* Corresponding authors.
E-mail addresses: alberto.spessa@polito.it (A. Spessa), alessandra.vitale@polito.it (A. Vitale).

https://doi.org/10.1016/j.porgcoat.2023.108098
Received 25 September 2023; Received in revised form 30 October 2023; Accepted 14 November 2023

photopolymerization-based 3D printing [24]. Also cyclic disulfides (e.g., 1,2-dithiolane) have been used in polymeric networks as photo-crosslinking agents [25,26].

Disulfide bonds are also a promising class of dynamic covalent bonds thanks to their high responsiveness to several external stimuli [23,27–29]. Regardless disulfide bonds possess a significant strength and a bond dissociation energy higher than other isostructural bonds, like peroxides or diselenides [16,30], they can be easily cleaved by temperature, pH, light, and redox conditions [30–32]. While aromatic disulfides can undergo exchange reaction even at room temperature, aliphatic ones need higher energy, and S—S exchange and recombination can be achieved by heating or irradiating the material [33–36]. This behavior can be exploited to provide the ability to repair mechanical damages: previous studies demonstrated how by applying heat [23,37–39] or light [28,40] either a scratch or a cut can be easily and successfully healed. Furthermore current research on self-healable materials is mainly focused on what are called "intrinsic materials" [41], in which self-healing is reached by introducing reversible covalent or non-covalent bonds into the monomer molecular chains [5,42].

In the coating field, providing a solution to obtain healing of surface damage has a primary importance: during their use, coatings are unavoidably prone to scratches, leading to a reduced lifespan and a loss of added value [5]. Therefore, the design and development of a UV-curable coating capable of self-healing have attracted increasing interest [27,43]. Some works already reported the exploitation of disulfide metathesis reaction for the self-healing of photocured polyurethane coatings [5,27,28]: high molecular weight polyurethane oligomers were prepared with a multistep synthetic process and an elastomeric behavior was obtained. Long treatment time and high temperatures were generally required for the self-healing of the coatings. In [23] a commercial acrylic disulfide is used as a comonomer with Bisphenol A bis(2-hydroxyl-3-methacryloxypropyl)ether obtaining a high Tg network which requires a thermal post curing and a harsh cycle for recovery the scratches.

In this work, with the aim of preparing a photoinitiator-free and self-healing UV-cured coating, we designed a novel polyurethane diacrylate monomer containing disulfide bonds requiring a simple synthetic procedure, i.e. a one step process. Its photopolymerization was investigated with or without a radical photoinitiator; clear UV-cured coatings were obtained, and the responsiveness of disulfide bonds was assessed by checking the healing of a surface scratch upon heating.

2. Materials and methods

2.1. Materials

2-Hydroxyethyl disulfide (HEDS), 2-acryloyloxyethyl isocyanate (AOI), 2,6-di-tert-butyl-4-methylphenol (BHT), and dibutyltin dilaurate (DBTL) were purchased from Sigma Aldrich. A photoinitiator blend (Genocure® LTM) of methylbenzoylformate (MBF) and 2,4,6-trimethylbenzoyldiphenyl phosphine oxide (TPO) was kindly supplied by Rahn AG, Switzerland.

All reagents were used without further purification. All other chemicals were purchased from Sigma-Aldrich.

2.2. Synthesis of disulfide-containing polyurethane diacrylate (DSPDA)

DSPDA was synthesized according to a well-established one-step acrylation reaction between a hydroxyl-terminated molecule and an acrylated isocyanate [44,45]. HEDS (88.29 g, 0.57 mol), BHT, and DBTL were added to a round-bottom reaction flask. The mixture was first stirred and then AOI (161.54 g, 1.14 mol) was inserted dropwise into the reaction flask by meaning of a graduated dropping funnel. A steady air inlet was fluxed inside the flask to avoid polymerization of the mixture. The exothermic reaction related to urethane bond formation was constantly monitored and kept in the range of 50–60 °C by cooling the system to avoid overheating of the mixture and thermal-induced cleavage of HEDS. The stirring continued until consumption of isocyanate groups, which presence in the reacting mixture was constantly monitored during the whole addition reaction between AOI and HEDS by means of FTIR. After one day in the container at room temperature, a wax-like compound was obtained, due to crystallization and hydrogen bond formation between urethane groups of the synthesized product.

The ^{1}H NMR and ^{13}C NMR spectra were recorded using a Magritek Spinsolve Multi-X ULTRA (^{1}H and ^{13}C), operating at 60 kHz dissolving samples in d-chloroform.

^{1}H NMR (60 MHz, $CDCl_3$): δ2.96 (t, 4H), δ3.47 (q, 4H), δ4.20–4.47 (m, 8H), δ5.20–5.60 (t, 2H), δ5.70–6.78 (m, 6H).

^{13}C NMR (60 MHz, $CDCl_3$): δ (ppm) 166.12, 156.48, 131.47, 128.20, 63.48, 62.76, 40.23, 37.30.

The molecular weight distribution of the synthesized product was investigated by performing a high-performance liquid chromatography (HPLC) using an Ultimate 3000 system (Thermo Scientific) equipped with an EC 125/4 Nucleodur 100-5 C18 column and an EC 4/2 Nucleodur 100-5 C18 precolumn. The column temperature was kept at 20 °C for the whole measurement. The mobile phase was acetonitrile/water (40:60 % v/v) and the injection volume was 2 µl. Detection was performed at a wavelength of 210 nm through the use of a UV–Vis spectrophotometer. Samples for analysis were prepared by diluting 100 mg HEDS or DSPDA in 10 ml of acetonitrile.

2.3. Coatings preparation

DSPDA with or without a photoinitiator (PI) was investigated. To prepare the formulation with the photoinitiator, first, DSPDA was heated up to 50 °C to allow melting. Once melted, 0.5 wt% of Genocure® LTM with respect to the monomer was added to liquid DSPDA and stirred at 50 °C for 15 min to ensure complete dispersion. Samples of DSPDA without PI and DSPDA with PI were kept at 50 °C, and thus in the liquid state, for the whole sample preparation process. Coatings were obtained by casting DSPDA with or without PI onto a glass slide with a 10 µm wire wound applicator. Coatings with a thickness of 50 µm were also prepared using the same procedure. Coatings were then cured using a high-pressure mercury-xenon lamp equipped with an optical fiber (LIGHTNINGCURE™ Spotlight source LC8, Hamamatsu), with an intensity of 90 mW cm^{-2} on the surface of the specimens, and fluxing N_2 gas. The UV light intensity was measured by a UV Power Puck® II (EIT® Instrument Markets). Samples were irradiated for 150 s to allow complete curing under an inert atmosphere. Since DSPDA solidifies at room temperature, coated glass slides were kept at 50 °C during the whole photocuring reaction.

2.4. Characterization

Photocleavage of disulfide-containing monomer was assessed using a 6850 Jenway UV–Vis spectrophotometer in absorbance mode, working in the range of 190–500 nm with a resolution of 0.2 nm. For irradiation experiments, DSPDA was dissolved in a suitable amount of anhydrous methanol to get a 5×10^{-4} M solution and placed into a 10 mm quartz cuvette. UV–Vis spectra were acquired before and after UV exposure at different times. Irradiation was performed with a medium-pressure Hg lamp (LIGHTNINGCURE™ Spotlight source LC8, Hamamatsu) exposing the sample to an intensity of 90 mW cm^{-2}. For comparison, a HEDS solution with a concentration of 1×10^{-3} M in methanol was prepared and tested in the same way.

UV–Vis spectroscopy on solid films was used as a method to evaluate the transparency of cured DSPDA coatings. Analyses were performed on 10 µm cured DSPDA samples detached from glass slide substrates and results were normalized concerning the thickness of the coating.

For evaluating the conversion of reactive groups during photopolymerization reaction, Fourier-transform Infrared (FTIR) spectroscopy analyses were performed, using a Thermo Fisher Scientific

Nicolet™ iS50 spectrometer in transmission mode in the spectral range of 4000–400 cm^{-1}. DSPDA films with a thickness of 10 μm were spread on a silicon wafer, heated up to 50 °C, irradiated for 150 s under an inert atmosphere (N_2), and analyzed by FT-IR spectroscopy, collecting 32 scans per spectrum with a resolution of 4 cm^{-1}. The conversion of the acrylate group was calculated using Eq. (1):

$$Conversion\% = (1 - A_t/A_0) \times 100 \quad (1)$$

where A_t is the area of the peak of the reactive group (acrylate C═C double bonds, at 1635 cm^{-1}) at time t of irradiation and A_0 is the area of the same peak before irradiation. The areas of such peaks were normalized to the area of the C═O stretch peak centered at 1720 cm^{-1}, used as an internal reference.

Photopolymerization reaction kinetics measurements were performed by real-time FTIR (rt-FTIR) spectroscopy through a Thermo Fisher Scientific Nicolet™ iS50 spectrometer in transmission mode, working in the spectral range of 2700–400 cm^{-1}. To prepare samples, DSPDA monomer samples were previously melted at 50 °C in the oven and then spread onto a silicon wafer using a 12 μm wire wound applicator. Irradiation of the samples was provided using the same high-pressure mercury-xenon lamp previously used, by placing the optical fiber 5 cm above the sample. The light intensity was 90 mW cm^{-2} on the surface of the sample, which was measured with a UV Power Puck® II radiometer (EIT® Instrument Markets). FTIR spectra were recorded continuously during irradiation, setting the sampling rate at 50 spectra per minute. To simulate an inert atmosphere around the sample, thus avoiding oxygen inhibition at the surface, films were covered with a 50 μm polyethylene film during measurements. The irradiation of the samples was performed for 150 s, switching on the UV lamp after 30 s from the beginning of the rt-FTIR measurements. For each sample (DSPDA without PI and DSPDA with PI), three different spectra were collected and then averaged in order to obtain the final conversion value at each irradiation time. The average standard deviation for each conversion curve was equal to 4 %. The photopolymerization rate was calculated as the first derivative of the double bond conversion versus time curve.

The insoluble fraction of photocured films was assessed by gel content analysis, evaluating the weight loss after 24 h of extraction in acetone at room temperature.

The synthesized monomer was characterized by differential scanning calorimetry (DSC), conducted with a Mettler Toledo DSC 3+, placing a total amount of 13.5 mg into a sealed aluminum pan. The uncured DSPDA sample was subjected to the following heating/cooling cycles, with a heating/cooling rate of 10 °C min^{-1}: a heating ramp from −70 to 60 °C, a cooling ramp from 60 to −70 °C, and a second heating ramp from −70 to 60 °C. The maximum temperature of 60 °C was set to avoid disulfide cleavage and monomer degradation during DSC analysis, which was performed under N_2 flux (50 ml min^{-1}). The glass transition temperature (T_g) was measured as the midpoint of the flex, while melting temperature (T_m) as the temperature corresponding to the maximum of the endothermic peak.

DSC measurements on photocured DSPDA samples were performed using Q20 TA Instruments, placing samples of about 5 mg in sealed aluminum pans. All the experiments performed were conducted under N_2 gas (50 ml min^{-1}). Samples were subjected to the following heating/cooling cycles: a heating ramp from −70 to 180 °C, a cooling ramp from 180 to −70 °C, and a second heating ramp from −70 to 180 °C. The heating/cooling rate for all the temperature ramps on all samples was set at 10 °C min^{-1}.

The wettability of DSPDA coatings was determined by performing static contact angle analysis by means of an FTA 1000C instrument (First Ten Angstroms) equipped with a video camera and an image analyzer. Five measurements were performed for each coating sample, calculating the mean value and error. The probe liquids used for contact angle analysis were water and hexadecane, whose surface tensions are 72.1 and 28.1 mN m^{-1}, respectively. For each sample, the surface energy was calculated according to the Owens-Wendt geometric mean method [46].

The color of 10 μm thick DSPDA coatings was investigated by performing spectrophotometric analysis, using a Datacolor Check II Plus spectrophotometer in reflectance mode under the condition of D65 illuminant and 10° standard observer. 10 μm coatings were detached from glass slides after curing and positioned onto a white paper for colorimetric analysis. The difference of color, reported as ΔE, between DSPDA without PI and DSPDA with PI coatings, was evaluated using the following equation (Eq. (2)):

$$\Delta E = \sqrt{(\Delta l)^2 + (\Delta a)^2 + (\Delta b)^2} \quad (2)$$

where L, a and b are color space coordinates, respectively lightness (black-white, L = 0 → L = 100), green-red (−a → +a), and blue-yellow coordinates (−b → +b). When ΔE value is lower than 3, the difference between the two colors cannot be recognized with the naked eye and is thus considered negligible.

Durometer hardness testing was used to measure the surface hardness of the DSPDA coatings. 50 μm thick DSPDA films with or without PI were tested with a portable AD-100-A Shore D Durometer (Checkline Europe BV). For each sample, three different measures were recorded and then averaged.

Solvent resistance of the 50 μm thick DSPDA cured coating was investigated using an adapted version of the ASTM D5402, rubbing the surface of the film with a cloth soaked with ethyl acetate. The solvent resistance was assessed as the number of double passes necessary to create a damage on the surface of the coating.

The self-healing ability of DSPDA samples was assessed by performing a scratch on the surface of the 10 μm thick coating employing a surgical blade and checking the healing after thermal treatment. Without applying any external forces, samples were placed into the oven either at 70 °C or 100 °C, and microscope images were taken after fixed time intervals. Optical microscope images were captured using an Olympus BX53MRF-S optical microscope with a magnification of 20×.

3. Results and discussion

3.1. Synthesis of disulfide-containing polyurethane diacrylate (DSPDA)

A novel disulfide-containing polyurethane diacrylated monomer (DSPDA) was synthesized through a conventional one-step addition reaction between HEDS and AOI [45]. The reaction scheme is shown in Scheme 1.

The chemical structure of synthesized DSPDA was investigated by ^1H NMR and ^{13}C NMR and the collected spectra are shown in Fig. 1. Analyzing the ^1H NMR spectrum (Fig. 1a), the multiplet present between δ 5.70 and δ 6.78 ppm was assigned to the proton attached to the acrylate group (−CH and $-CH_2$). The absorption peaks in δ 5.20 and δ 5.60 ppm region were assigned to amide-related hydrogens, part of urethane linkage. The absorption peaks at δ 4.20 - δ 4.47 ppm were due to the proton on the α-position methylene ($-CH_2$) next to the ester group. Quartet given by protons on α-position methylene ($-CH_2$) next to amide was found at δ 3.47 ppm. Absorption peaks at δ 2.96 ppm were assigned to α-position methylene ($-CH_2$) with respect to the disulfide bond. To further confirm the chemical structure of the DSPDA monomer, ^{13}C NMR spectroscopy was conducted (Fig. 1b). The peak related to ester −COO appeared at δ 166.12 ppm and the urethane-related −NCOO peak was observed at δ 156.48 ppm. Acrylate carbon double bond C═C was found at δ 131.47 and δ 128.20 ppm, respectively. Aliphatic $-CH_2$ peaks were observed at δ 63.48, δ 62.76 ppm and δ 40.23, δ 37.30 ppm. All these results indicated that the structure of the synthesized disulfide-containing monomer was consistent with the hypothesized one.

HPLC was performed on both samples of HEDS and synthesized DSPDA monomer to further confirm the yield, and thus the success, of the addition reaction between HEDS and AOI. By looking at the

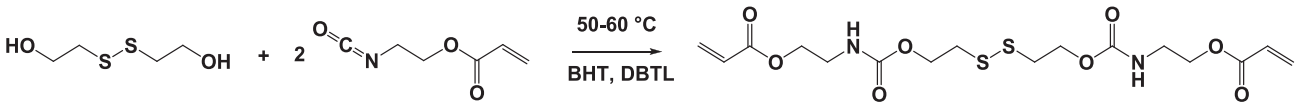

Scheme 1. Synthesis route of DSPDA.

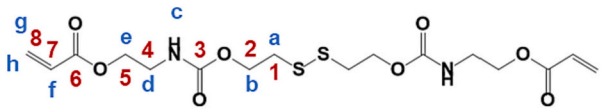

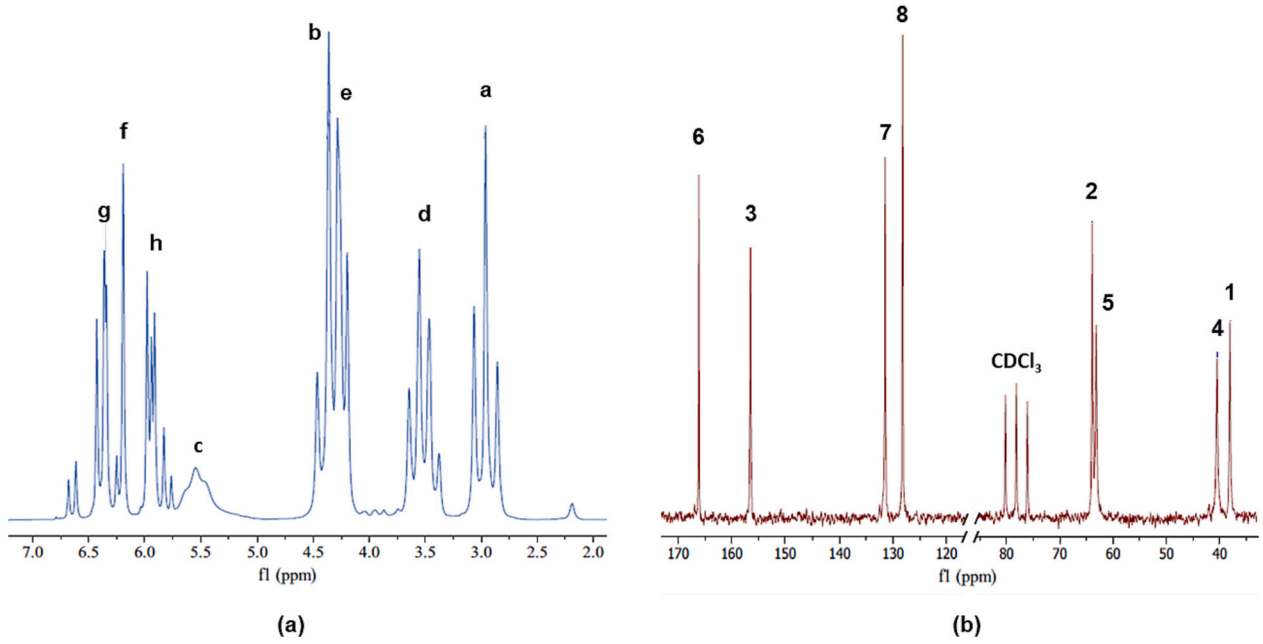

Fig. 1. (a) ^{1}H NMR and (b) ^{13}C NMR of DSPDA monomer.

chromatogram of DSPDA (Fig. 2), different peaks could be highlighted, each one referring to a different synthesis product. The comparison with the chromatogram of HEDS was used to assign the peaks related to the synthesized monomer, while ratios between areas were used to calculate the relative amount of each species. The more intense peak around 6 min was assigned to the desired product, in which the addition reaction occurred on both hydroxyl groups of HEDS. The relative amount for this product is the highest, accounting for around 84 %. The smaller peaks at 4.2 min was reasonably referred to the monosubstituted HEDS, with a relative percentage of around 11 %. Low intensity peaks between 1.6 min and 3 min, which in total count for 5 %, were probably given by impurities, since no unreacted HEDS was present after the synthesis reaction, as confirmed by the absence of a peak at 1.2 min corresponding to HEDS in the final DSPDA chromatogram. Even if a small amount of mono-substituted monomer remained after the addition reaction, a huge amount of disubstituted DSPDA could be obtained, confirming the efficiency and the high yield of this synthesis strategy. Moreover, the absence of other peaks in the elugram further supported the necessity of controlling the exothermic reaction to avoid byproducts generation during synthesis.

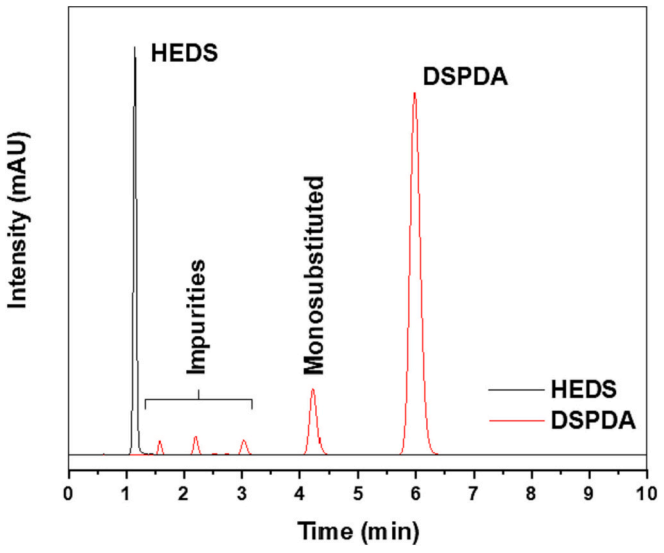

Fig. 2. HPLC chromatogram of HEDS (black curve) and DSPDA monomer after synthesis (red curve). (For interpretation of the references to color in this figure legend, the reader is referred to the web version of this article.)

The thermal transitions and characteristic temperatures of the DSPDA monomer were investigated using DSC. As can be observed in Fig. 3, the T_g was −35.6 °C, while the T_m was around 43.1 °C. The exothermic peak before melting at 26.7 °C could be ascribed to the cold crystallization of monomer chains, given by the formation of hydrogen bonds between urethane groups present in DSPDA. Due to this crystallization, DSPDA appeared as a whitish wax-like solid at room temperature.

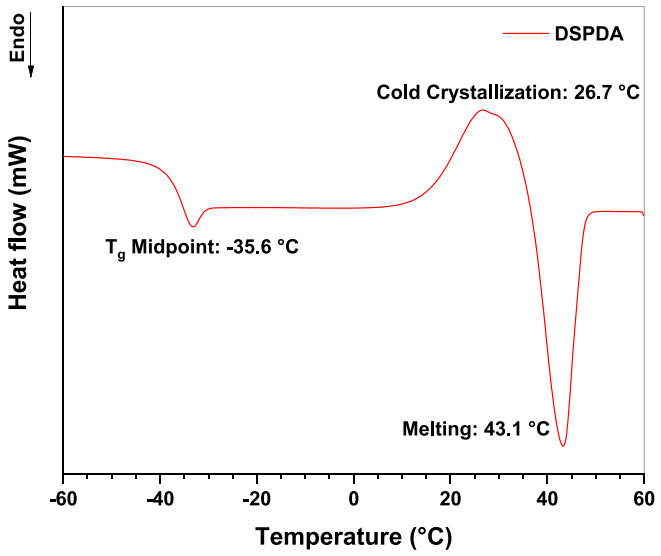

Fig. 3. DSC curve of DSPDA monomer.

3.2. Photopolymerization reaction

First, the disulfide bond photocleavage of HEDS and DSPDA was investigated by UV–Vis spectroscopy of their solutions in methanol. As can be seen from Fig. 4, an absorption peak at 249 nm was present in both spectra, which was assigned to n → σ* electronic transition of the S—S bond [18,20]. Its molar absorption coefficients were 3.13×10^2 M^{-1} cm^{-1} and 5.80×10^2 M^{-1} cm^{-1} for HEDS and DSPDA, respectively. The solutions were then irradiated with UV light: spectra after 15 s and 150 s of irradiation are reported in Fig. 4. Upon irradiation, a decrease in peak intensity was seen, demonstrating that S—S bonds were cleaved under UV light forming thiyl radicals.

To evaluate the initiation ability of thiyl radicals generated by DSPDA photocleavage, and thus its self-polymerization, the photocuring of the monomer alone (DSPDA without PI) was studied by FTIR spectroscopy. In parallel, as a comparison, the photopolymerization of DSPDA added of a typical photoinitiator (DSPDA with PI) was also investigated. The extent of the crosslinking of acrylate moieties, and thus conversion, was monitored by looking at the decrease of the C═C double bond absorption peaks at 1635 cm^{-1} upon irradiation. According to data reported in Fig. 5, for both samples, after irradiation the acrylate characteristic absorption peak strongly decreased, indicating an almost complete crosslinking reaction between terminal acrylate groups of DSPDA. As previously demonstrated by UV–Vis analysis and as widely reported in the literature [16–20,25,26], disulfide bonds present in DSPDA molecules were cleaved by UV light exposure forming thiyl radicals, which are able to start the polymerization of acrylate groups [21]. Notably, pure monomer without any addition of photoinitiator achieved a conversion value similar to the one reached for the sample containing a commercial photoinitiator: as reported in Table 1, when irradiation was carried out for 150 s at room temperature under an inert atmosphere, a remarkable conversion of double bonds of around 85 % was reached for both samples, with and without PI. These results revealed that reactive thiyl radicals generated by photocleavage of DSPDA were able to start the photopolymerization reaction, as illustrated in Scheme 2 (Path II), reaching a level of conversion significantly higher than those found in the literature for similar acrylated disulfide molecules [22].

The photopolymerization kinetics was evaluated by real-time FTIR (rt-FTIR) analyses: conversion curves and related polymerization rates are reported in Fig. 6. Despite the similar degree of conversion, the two DSPDA samples (i.e., with and without PI) had different polymerization rates. The rate of the reaction was obviously enhanced by adding LTM photoinitiator to the system and, as reported in Fig. 6b, the peak reached 19 % s^{-1}, a value definitely higher than the one for DSPDA without PI (12 % s^{-1}). However, all these findings demonstrate the excellent ability of DSPDA monomer to successfully self-initiate the photopolymerization reaction.

The photopolymerization of DSPDA was strongly influenced by crystallization phenomena. At room temperature, DSPDA appeared as a whitish wax-like solid crystal and had to be melted prior to irradiation to allow the formation of a clear film. Since the melting temperature of DSPDA was 43.1 °C when photopolymerization was performed on DSPDA at room temperature, crystallization occurred, competing with network formation. Due to this phenomenon, the mobility of DSPDA molecules and growing polymeric chains was reduced, slowing the crosslinking reaction and thus the conversion of acrylic double bonds. This hypothesis was confirmed by heating the monomer with and without PI at 50 °C during irradiation and measuring their C═C conversion by FTIR analyses. When DSPDA samples were maintained above crystallization temperature during the whole photocuring process, the degree of conversion increased for both samples and reached values of 92 % and 94 % for DSPDA without PI and DSPDA with PI, respectively (Table 1). By heating the samples the mobility of chains was enhanced and crystallization did not occur, allowing a higher degree of conversion for the coating.

Finally, in order to control the condition of disulfide bonds after

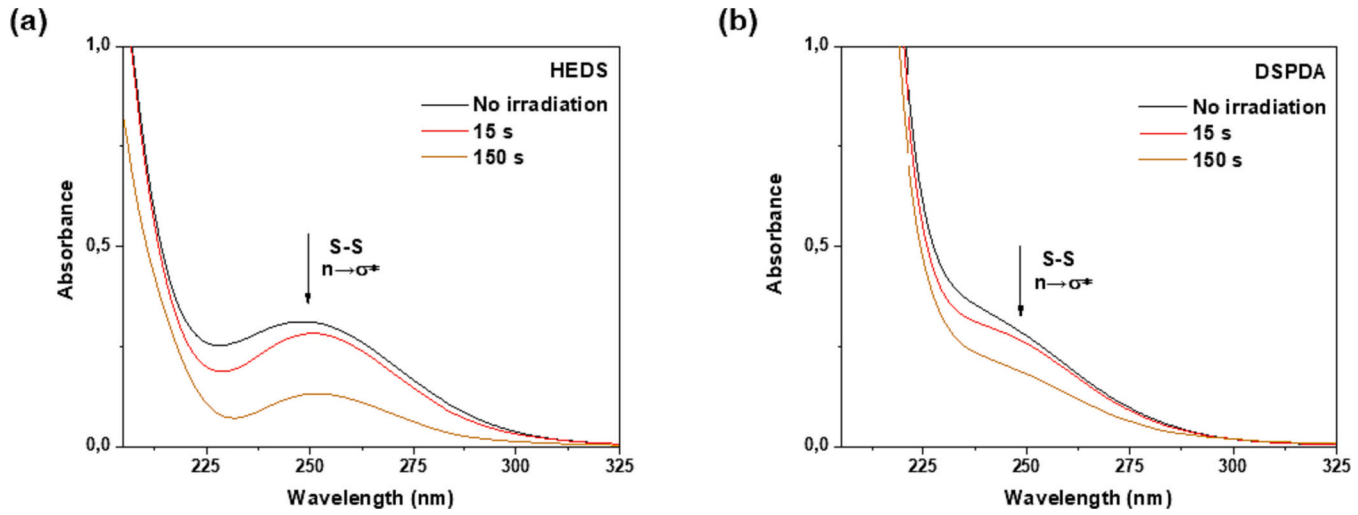

Fig. 4. UV–Vis photolysis spectra of (a) HEDS 5×10^{-4} M and (b) DSPDA 1×10^{-3} M solutions in anhydrous methanol.

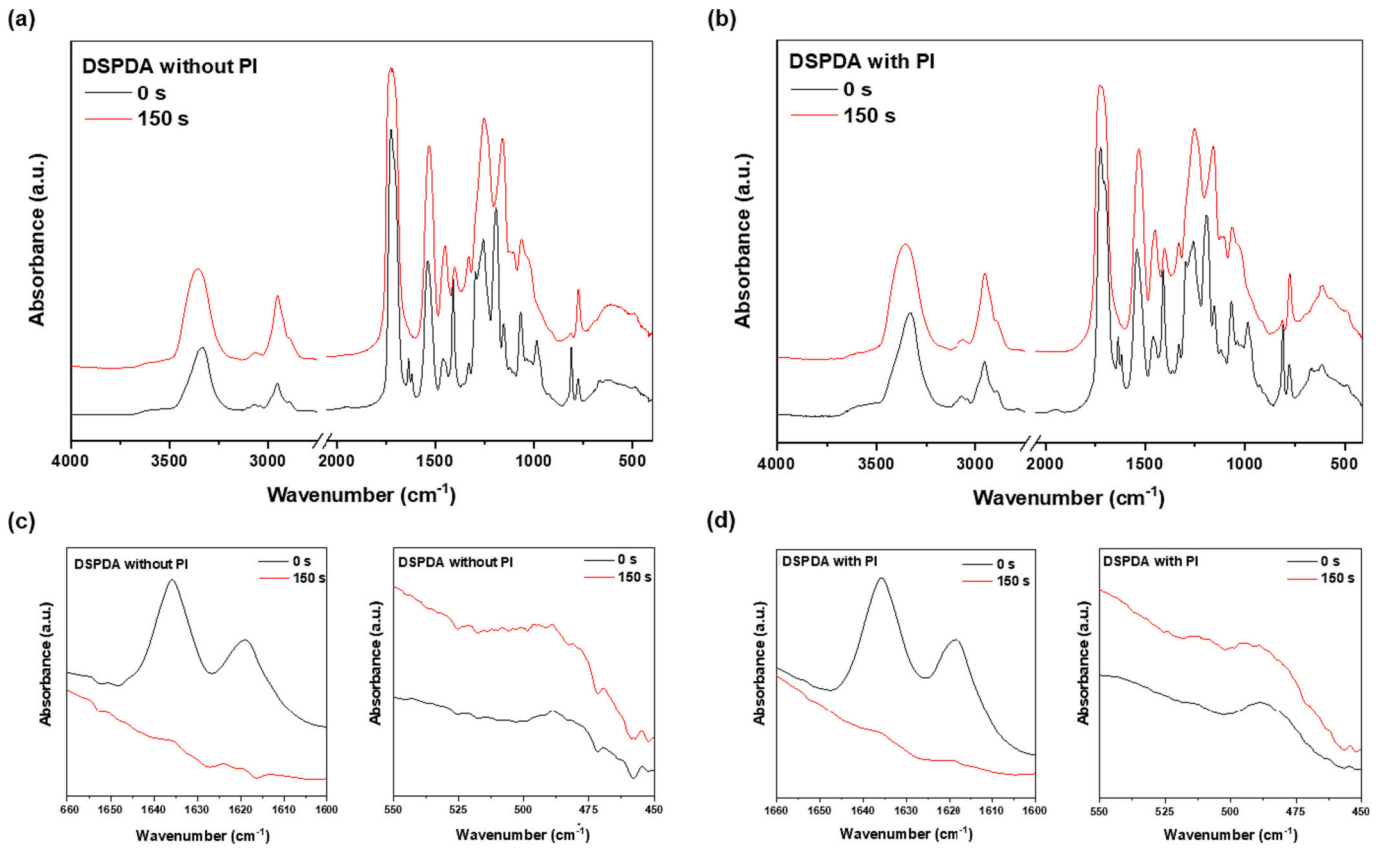

Fig. 5. FTIR spectra of (a) DSPDA without PI and (b) DSPDA with PI, before (0 s) and after (150 s) light irradiation. Close-ups on C═C and S—S stretching peaks for (c) DSPDA without PI and (d) DSPDA with PI are also reported.

Table 1
Double bond conversion of DSPDA coating at different temperatures, measured by FTIR spectroscopic analyses.

Sample	Double bond conversion, RT [%]	Double bond conversion, 50 °C [%]
DSPDA without PI	86	92
DSPDA with PI	85	94

photocuring of the monomer, in the FTIR spectra, the low-intensity peak between 475 and 500 cm^{-1} related to S—S stretching vibration [47] was monitored (Fig. 5c and d). The presence of this band was used just as a qualitative tool, due to the weakness of absorption of such vibration. As previously discussed, photocleavage of disulfide occurred during the photopolymerization reaction, leading to the generation of thiyl radicals. In contrast with this finding, the S—S stretching peak could be found both before and after irradiation in the FTIR spectra. It may be assumed that even if thiyl radicals were produced due to UV light exposure, disulfide bonds were promptly reformed between radicals not involved in the initiation reaction. A scheme of the proposed reaction mechanism is reported in Scheme 2.

3.3. Coating characterization

Since the synthesized monomer could be photocured even without the presence of a photoinitiator, DSPDA with and without PI films were characterized as a potential thin coating for different applications.

First, gel fraction analyses were performed on DSPDA coatings to cross-check the photocrosslinking conversions results, by extracting unreacted monomer with a 24 h treatment in acetone: data are reported in Table 2. Similar values were obtained for DSPDA without PI and DSPDA with PI, respectively 95 % and 97 % of gel, confirming the efficiency of the photocuring reaction even in the absence of the photoinitiator.

The transparency of the coatings was evaluated through UV–Vis spectroscopy. As it is evident from Fig. 7, almost 100 % transmittance was registered between 400 nm and 750 nm for both samples, highlighting no relevant differences between DSPDA without PI and DSPDA with PI coatings in the visible region. Transparency and clearness of coatings could also be qualitatively appreciated by the naked eye by looking at the coated glass slides in Fig. 8. Despite the similar transmittance values for wavelengths higher than 400 nm, the two DSPDA samples revealed a striking difference in the UV region. The DSPDA sample containing the photoinitiator showed a strong decrease in transmittance value, due to the high light absorption of photoproducts in that specific region. In contrast, DSPDA without PI specimens exhibited only a negligible absorption band around 250 nm, ascribable to disulfide bonds present in the network.

The color of the coatings was also evaluated, focusing on a color effect given by the presence of photoproducts after curing the sample with photoinitiator, with respect to the one without. The difference in the color was calculated from ΔE value, as explained in the Experimental section. Starting from L, a, and b parameters obtained with a datacolor for both samples (data reported in Table 2), a ΔE of 0.47 was calculated, indicating a negligible difference between the color of DSPDA with and without PI coatings.

The thermal properties of crosslinked DSPDA films were evaluated

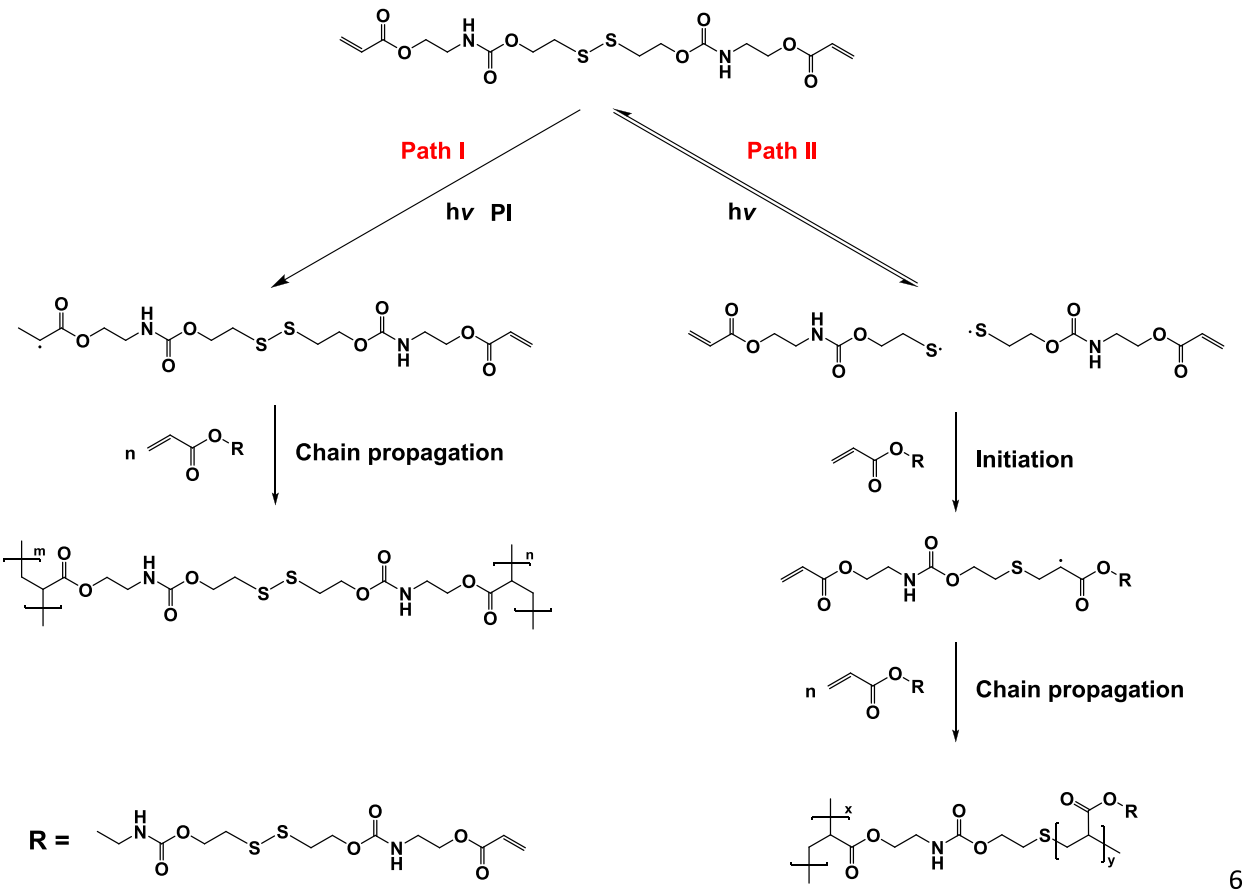

Scheme 2. Reaction mechanisms proposed for DSPDA during photopolymerization reaction: in the presence of a photoinitiator (Path I) and in the absence of a photoinitiator (i.e., self-initiating reaction, Path II).

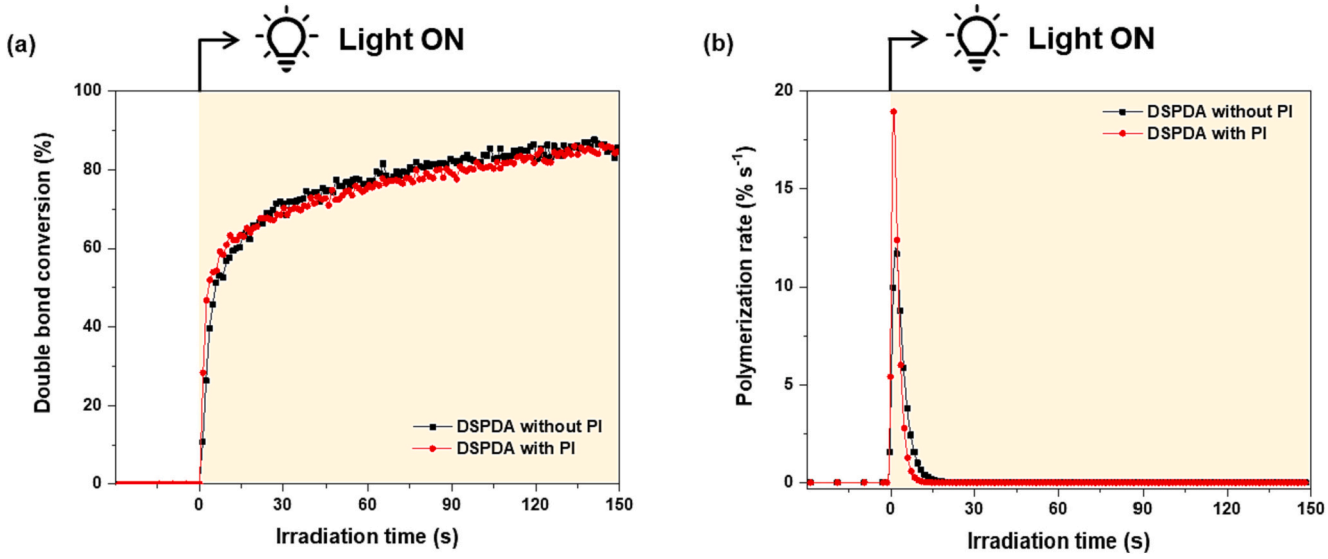

Fig. 6. Photocuring kinetics curves of DSPDA samples in the presence or absence of photoinitiator. (a) Conversion of acrylate double bonds over irradiation time and (b) polymerization rate over irradiation time.

by DSC analysis. According to data shown in Table 2, the addition of the photoinitiator to DSPDA monomer causes a slight increase in the glass transition temperature of the photocured coating, shifting the value from 72.6 °C to 84.2 °C. This minimal difference between T_g values could be referred to different networks obtained after photocuring. When thiyl radicals are produced, shorter molecules undergo crosslinking reaction (Scheme 2, Path II), bringing a change in the size of the network meshes as can be deduced from the proposed reaction mechanism. In contrast, the presence of the photoinitiator, in addition to a higher acylate conversion, reduced the use of thiyl radicals favoring the recombination of disulfide bonds, thus increasing the amount of longer molecules that undergo crosslinking reaction (Scheme 2, Path I).

Table 2
Gel fraction, colorimetric values, glass transition temperature, contact angles of water and hexadecane with the respective surface energies and components, Shore hardness, and solvent resistance values of DSPDA with or without PI.

	DSPDA without PI	DSPDS with PI
Gel fraction [%]	95	97
L, a, b	87.24, 2.51, −11.08	87.15, 2.42, −10.63
T_g [°C]	72.6	84.2
θ_w [°]	65.4 ± 0.9	65.4 ± 3.3
θ_h [°]	6.3 ± 0.4	6.4 ± 0.4
γ_S [mN m^{-1}]	41.7	41.7
γ_S^D [mN m^{-1}]	27.3	27.3
γ_S^P [mN m^{-1}]	14.4	14.4
Shore hardness [D]	88 ± 2	91 ± 1
Solvent resistance [# double passes]	30	50

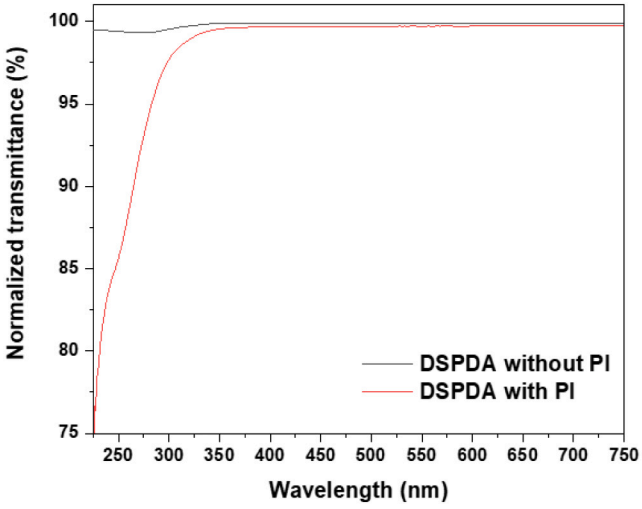

Fig. 7. UV–Vis spectra of photocured coatings made of DSPDA without and with photoinitiator.

The wettability of DSPDA coatings was assessed through contact angle analyses, using both a polar (water) and an apolar (hexadecane) solvent: contact angle values obtained are reported in Table 2. Based on average collected values, no substantial difference could be highlighted between the sample containing the photoinitiator and the one made with pure DSPDA. The water contact angle values (θ_w) obtained were in the expected range for an acrylate network [48,49], while contact angles obtained with hexadecane (θ_h) demonstrated the high lipophilicity of DSPDA films. Using these data, the surface energy γ_S of the coatings, together with its dispersive (γ_S^D) and polar (γ_S^P) components, was calculated (Table 2). As expected, the same values were obtained for the coatings with and without PI, completely in accordance with typical acrylic coatings.

The surface hardness of the coating was investigated with a shore durometer: the obtained D hardness values are reported in Table 2. As already seen for other properties of the coating, the difference between the values recorded for the system containing PI and the one without PI was negligible, being 91 ± 1 and 88 ± 2 D respectively.

Finally, the solvent resistance of the photocured coatings was evaluated by the rub test. Differently, the rub test returned more deviant results, reported in Table 2, assessing the solvent resistance value of DSPDA coating with PI and without PI respectively at 50 double passes and 30 double passes: this value is lower than industrial level, where more than 100 double passes resistance is usually required.

All the collected results were in accordance with the previous reported gel fractions and T_g values, and the differences could be referred to the different conversion degree and the formation of a different network in the case of the self-initiated photocuring of pure DSPDA.

3.4. Self-healing of the coatings

As discussed above, the spectroscopic results on the coatings after irradiation (Fig. 5) showed that disulfide bonds were still present inside the polymeric network even after photocrosslinking of DSPDA samples. Therefore, photocured coatings were evaluated for self-healing ability after being scratched with a surgical blade. Due to heat-induced disulfide metathesis reaction, the acrylic network can be self-healed when sufficient energy is provided to allow cleavage and recombination of the disulfide bonds. A qualitative analysis of the self-healing behavior of DSPDA coatings for repairing surface scratches was conducted by looking at the samples before and after thermal treatment with an optical microscope. First, a self-healing test was performed by heating samples at 70 °C in the oven, to assess its healing ability even at a temperature slightly below T_g. After 24 h of thermal treatment, scratches were still present on the surface of the coatings and only a minimal improvement on the least deep damages could be highlighted with optical analyses.

The results remarkably changed when the test was performed at 100 °C, i.e., at a temperature higher than the glass transition temperature of the films, allowing a higher movement of the polymeric chains during the healing treatment. As depicted in Fig. 9, after only 10 min at 100 °C, scratches on the surface of the coatings were completely healed, while the surrounding region remained unchanged as confirmed by the presence of defects in the films in both images. Compared to self-healing conditions of other disulfide-containing materials described in previous works [35,39] (i.e., which had a T_g lower than 0 °C), in the case of DSPDA the healing of surface scratches occurred even when samples were heated around 20 °C above glass transition temperature, avoiding the necessity of overheating the samples to reach the curing. Considering disulfide-containing coatings with a high glass transition temperature [23], DSPDA films could be healed in a shorter time, mainly thanks to the high amount of disulfide-bonds present, producing an almost complete removal of surface scratches after a few minutes of treatment. Reasonably, the high amount of dynamic disulfide linkages present in the final DSPDA network, could be highlighted as the main reason for the good self-healing ability reached by DSPDA coating. Lastly,

Fig. 8. Images of photocured DSPDA coatings (approximately 10 μm thick) on glass slides.

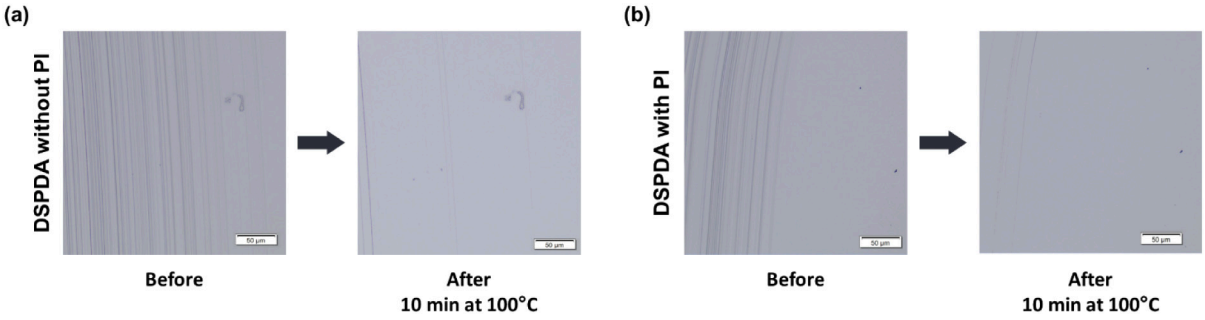

Fig. 9. Image of scratched surface of (a) DSPDA without PI and (b) DSPDA with PI, before and after the thermal treatment at 100 °C for 10 min.

comparing the performance of DSPDA with and without PI, no substantial difference was detected and in both cases was reached an almost complete heal of the scratched part.

4. Conclusions

Herein, a disulfide-containing polyurethane diacrylate (DSPDA) monomer was successfully synthesized through a simple and straightforward one step process. It was used to produce a novel clear self-initiating and self-healable coating. Under UV irradiation, DSPDA undergoes cleavage of disulfide linkages, leading to the production of thiyl radicals. These radicals are either able to recombine, recovering the S—S bonds, or to attack acrylate double bonds starting polymerization. Accordingly, DSPDA exhibited high double bond conversion (92 %) and gel fraction (95 %) even without a photoinitiator, albeit with a lower polymerization rate than in its presence. DSPDA gave transparent coatings with high surface hardness either in the presence or in the absence of a photoinitiator. The self-healing ability of DSPDA samples was assessed, and results showed how the healing of the coating could be reached in mild conditions, after a relatively short thermal treatment of 10 min at 100 °C, i.e., at a temperature higher than T_g.

Overall, the results provide new insights and opportunities into the design, synthesis, and use of disulfide-containing monomers for UV-curable coating. Remarkably, the use of DSPDA brings not only to the development of a clear, self-healable material but also to a self-initiating photocuring process, avoiding the use of a photoinitiator and all the issues related, first among them the presence of photoproducts in the final cured coating.

CRediT authorship contribution statement

Alberto Spessa: Conceptualization, Methodology, Investigation, Writing – original draft, Visualization. **Roberta Bongiovanni:** Conceptualization, Methodology, Writing – review & editing, Resources, Supervision, Project administration. **Alessandra Vitale:** Conceptualization, Methodology, Writing – review & editing, Resources, Supervision, Project administration.

Declaration of competing interest

The authors declare no competing financial interest or personal relationship that could have appeared to influence the work reported in this paper.

Data availability

Data will be made available on request.

Acknowledgments

Funding: This work was supported by the Italian Ministry of University and Research (MUR) [DM 1061/2021 PON-Dottorati di ricerca su tematiche green e dell'innovazione].

References

[1] A. Vitale, S. Molina-Gutiérrez, W.S.J. Li, S. Caillol, V. Ladmiral, P. Lacroix-Desmazes, S. Dalle Vacche, Biobased composites by photoinduced polymerization of cardanol methacrylate with microfibrillated cellulose, Materials 15 (2022) 339, https://doi.org/10.3390/ma15010339.
[2] S. Molina-Gutiérrez, S. Dalle Vacche, A. Vitale, V. Ladmiral, S. Caillol, R. Bongiovanni, P. Lacroix-Desmazes, Photoinduced polymerization of eugenol-derived methacrylates, Molecules 25 (2020) 3444, https://doi.org/10.3390/molecules25153444.
[3] Y. Yagci, S. Jockusch, N.J. Turro, Photoinitiated polymerization: advances, challenges, and opportunities, Macromolecules 43 (2010) 6245–6260, https://doi.org/10.1021/ma1007545.
[4] E. Rossegger, Y. Li, H. Frommwald, S. Schlögl, Vat photopolymerization 3D printing with light-responsive thiol-norbornene photopolymers, Monatsh. Chem. 154 (2023) 473–480, https://doi.org/10.1007/s00706-022-03016-5.
[5] Y. Zhang, Y. Sheng, M. Wang, X. Lu, UV-curable self-healing, high hardness and transparent polyurethane acrylate coating based on dynamic bonds and modified nano-silica, Prog. Org. Coat. 172 (2022), 107051, https://doi.org/10.1016/j.porgcoat.2022.107051.
[6] Z. Guo, Research advances in UV-curable self-healing coatings, RSC Adv. 12 (2022) 32429–32439, https://doi.org/10.1039/D2RA06089B.
[7] J.P. Fouassier, J. Lalevée, Photoinitiators Structures, Reactivity and Applications in Polymerization, Wiley-VCH Verlag GmbH & Co. KGaA, Weinheim, Germany, 2021.
[8] R. Bongiovanni, S.D. Vacche, A. Vitale, Photoinduced processes as a way to sustainable polymers and innovation in polymeric materials, Polymers 13 (2021) 2293, https://doi.org/10.3390/polym13142293.
[9] M. Zhang, S. Jiang, Y. Gao, J. Nie, F. Sun, Design of a disulfide bond-containing photoresist with extremely low volume shrinkage and excellent degradation ability for UV-nanoimprinting lithography, Chem. Eng. J. 390 (2020), 124625, https://doi.org/10.1016/j.cej.2020.124625.
[10] T. Scherzer, VUV-induced photopolymerization of acrylates, Macromol. Chem. Phys. 213 (2012) 324–334, https://doi.org/10.1002/macp.201100485.
[11] O. Daikos, S. Naumov, W. Knolle, K. Heymann, T. Scherzer, Peculiarities of the photoinitiator-free photopolymerization of pentabrominated and pentafluorinated aromatic acrylates and methacrylates, Phys. Chem. Chem. Phys. 18 (2016) 32369–32377, https://doi.org/10.1039/C6CP06549J.
[12] F. Karasu, C. Dworak, S. Kopeinig, E. Hummer, N. Arsu, R. Liska, Photoinitiating monomers based on diacrylamides, Macromolecules 41 (2008) 7953–7958, https://doi.org/10.1021/ma8017537.
[13] R. Bongiovanni, M. Sangermano, G. Malucelli, A. Priola, UV curing of photoinitiator-free systems containing bismaleimides and diacrylate resins: bulk and surface properties, Prog. Org. Coat. 53 (2005) 46–49, https://doi.org/10.1016/j.porgcoat.2004.11.009.
[14] N.B. Cramer, J.P. Scott, C.N. Bowman, Photopolymerizations of thiol−Ene polymers without photoinitiators, Macromolecules 35 (2002) 5361–5365, https://doi.org/10.1021/ma0200672.
[15] C.E. Hoyle, C.N. Bowman, Thiol-ene click chemistry, Angew. Chem. Int. Ed. 49 (2010) 1540–1573, https://doi.org/10.1002/anie.200903924.
[16] S.M. Soars, N.J. Bongiardina, B.D. Fairbanks, M. Podgórski, C.N. Bowman, Spatial and temporal control of photomediated disulfide–ene and thiol–ene chemistries for two-stage polymerizations, Macromolecules 55 (2022) 1811–1821, https://doi.org/10.1021/acs.macromol.1c02464.
[17] M. Teders, C. Henkel, L. Anhäuser, F. Strieth-Kalthoff, A. Gómez-Suárez, R. Kleinmans, A. Kahnt, A. Rentmeister, D. Guldi, F. Glorius, The energy-transfer-enabled biocompatible disulfide–ene reaction, Nat. Chem. 10 (2018) 981–988, https://doi.org/10.1038/s41557-018-0102-z.
[18] C.W. Bookwalter, D.L. Zoller, P.L. Ross, M.V. Johnston, Bond-selective photodissociation of aliphatic disulfides, J. Am. Soc. Mass Spectrom. 6 (1995) 872–876, https://doi.org/10.1016/1044-0305(95)00483-T.
[19] H.M. Dizman, N. Arsu, Rapid and sensitive colorimetric determination of dopamine and serotonin in solution and polymer matrix with photochemically prepared and

N-acetyl-L-cysteine functionalized gold nanoparticles, Mater. Today Commun. 35 (2023), 105599, https://doi.org/10.1016/j.mtcomm.2023.105599.
[20] A. Chemtob, N. Feillée, C. Vaulot, C. Ley, D. Le Nouen, Self-photopolymerization of poly(disulfide) oligomers, ACS Omega 4 (2019) 5722–5730, https://doi.org/10.1021/acsomega.9b00021.
[21] J. Chen, S. Jiang, Y. Gao, F. Sun, Reducing volumetric shrinkage of photopolymerizable materials using reversible disulfide-bond reactions, J. Mater. Sci. 53 (2018) 16169–16181, https://doi.org/10.1007/s10853-018-2778-2.
[22] M. Zhang, S. Jiang, Y. Gao, J. Nie, F. Sun, UV-nanoimprinting lithography photoresists with no photoinitiator and low polymerization shrinkage, Ind. Eng. Chem. Res. 59 (2020) 7564–7574, https://doi.org/10.1021/acs.iecr.9b07103.
[23] L.M. Sáiz, M.G. Prolongo, V. Bonache, A. Jiménez-Suárez, S.G. Prolongo, Self-healing materials based on disulfide bond-containing acrylate networks, Polym. Test. 117 (2023), 107832, https://doi.org/10.1016/j.polymertesting.2022.107832.
[24] X. Li, R. Yu, Y. He, Y. Zhang, X. Yang, X. Zhao, W. Huang, Self-healing polyurethane elastomers based on a disulfide bond by digital light processing 3D printing, ACS Macro Lett. 8 (2019) 1511–1516, https://doi.org/10.1021/acsmacrolett.9b00766.
[25] B. Sieredzinska, Q. Zhang, K.J. van den Berg, J. Flapper, B.L. Feringa, Photo-crosslinking polymers by dynamic covalent disulfide bonds, Chem. Commun. 57 (2021) 9838–9841, https://doi.org/10.1039/D1CC03648C.
[26] S. Maes, V. Scholiers, F.E. Du Prez, Photo-crosslinking and reductive decrosslinking of polymethacrylate-based copolymers containing 1,2-dithiolane rings, Macro Chem. Phys. 224 (2022) 8, https://doi.org/10.1002/macp.202100445.
[27] T. Li, Z.P. Zhang, M.Z. Rong, M.Q. Zhang, Self-healable and thiol–ene UV-curable waterborne polyurethane for anticorrosion coating, J. Appl. Polym. Sci. 136 (2019), 47700, https://doi.org/10.1002/app.47700.
[28] D. Zhao, S. Liu, Y. Wu, T. Guan, N. Sun, B. Ren, Self-healing UV light-curable resins containing disulfide group: synthesis and application in UV coatings, Prog. Org. Coat. 133 (2019) 289–298, https://doi.org/10.1016/j.porgcoat.2019.04.060.
[29] J.M. Matxain, J.M. Asua, F. Ruipérez, Design of new disulfide-based organic compounds for the improvement of self-healing materials, Phys. Chem. Chem. Phys. 18 (2016) 1758–1770, https://doi.org/10.1039/C5CP06660C.
[30] F. Dénès, M. Pichowicz, G. Povie, P. Renaud, Thiyl radicals in organic synthesis, Chem. Rev. 114 (2014) 2587–2693, https://doi.org/10.1021/cr400441m.
[31] G. Deng, F. Li, H. Yu, F. Liu, C. Liu, W. Sun, H. Jiang, Y. Chen, Dynamic hydrogels with an environmental adaptive self-healing ability and dual responsive sol–gel transitions, ACS Macro Lett. 1 (2012) 275–279, https://doi.org/10.1021/mz200195n.
[32] L. Zhang, L. Chen, S.J. Rowan, Trapping dynamic disulfide bonds in the hard segments of thermoplastic polyurethane elastomers, Macromol. Chem. Phys. 218 (2017), 1600320, https://doi.org/10.1002/macp.201600320.
[33] A. Rekondo, R. Martin, A. Ruiz De Luzuriaga, G. Cabañero, H.J. Grande, I. Odriozola, Catalyst-free room-temperature self-healing elastomers based on aromatic disulfide metathesis, Mater. Horiz. 1 (2014) 237–240, https://doi.org/10.1039/C3MH00061C.
[34] L. Li, W. Feng, A. Welle, P.A. Levkin, UV-induced disulfide formation and reduction for dynamic photopatterning, Angew. Chem. Int. Ed. 55 (2016) 13765–13769, https://doi.org/10.1002/anie.201607276.
[35] J. Canadell, H. Goossens, B. Klumperman, Self-healing materials based on disulfide links, Macromolecules 44 (2011) 2536–2541, https://doi.org/10.1021/ma2001492.
[36] H. Otsuka, S. Nagano, Y. Kobashi, T. Maeda, A. Takahara, A dynamic covalent polymer driven by disulfide metathesis under photoirradiation, Chem. Commun. 46 (2010) 1150–1152, https://doi.org/10.1039/B916128G.
[37] I. Azcune, I. Odriozola, Aromatic disulfide crosslinks in polymer systems: self-healing, reprocessability, recyclability and more, Eur. Polym. J. 84 (2016) 147–160, https://doi.org/10.1016/j.eurpolymj.2016.09.023.
[38] L. Imbernon, E.K. Oikonomou, S. Norvez, L. Leibler, Chemically crosslinked yet reprocessable epoxidized natural rubber via thermo-activated disulfide rearrangements, Polym. Chem. 6 (2015) 4271–4278, https://doi.org/10.1039/C5PY00459D.
[39] L. Ling, J. Li, G. Zhang, R. Sun, C.-P. Wong, Self-healing and shape memory linear polyurethane based on disulfide linkages with excellent mechanical property, Macromol. Res. 26 (2018) 365–373, https://doi.org/10.1007/s13233-018-6037-9.
[40] W.M. Xu, M.Z. Rong, M.Q. Zhang, Sunlight driven self-healing, reshaping and recycling of a robust, transparent and yellowing-resistant polymer, J. Mater. Chem. A 4 (2016) 10683–10690, https://doi.org/10.1039/C6TA02662A.
[41] F. Gao, J. Cao, Q. Wang, R. Liu, S. Zhang, J. Liu, X. Liu, Properties of UV-cured self-healing coatings prepared with PCDL-based polyurethane containing multiple H-bonds, Prog. Org. Coat. 113 (2017) 160–167, https://doi.org/10.1016/j.porgcoat.2017.09.011.
[42] M. Liu, J. Zhong, Z. Li, J. Rong, K. Yang, J. Zhou, L. Shen, F. Gao, X. Huang, H. He, A high stiffness and self-healable polyurethane based on disulfide bonds and hydrogen bonding, Eur. Polym. J. 124 (2020), 109475, https://doi.org/10.1016/j.eurpolymj.2020.109475.
[43] W. Gao, M. Bie, Y. Quan, J. Zhu, W. Zhang, Self-healing, reprocessing and sealing abilities of polysulfide-based polyurethane, Polymer 151 (2018) 27–33, https://doi.org/10.1016/j.polymer.2018.07.047.
[44] R. Bongiovanni, A. Medici, A. Zompatori, S. Garavaglia, C. Tonelli, Perfluoropolyether polymers by UV curing: design, synthesis and characterization, Polym. Int. 61 (2012) 65–73, https://doi.org/10.1002/pi.3149.
[45] Y. Liu, S. Li, L. Feng, H. Yu, X. Qi, W. Wei, J. Li, W. Dong, Novel disulfide-containing poly(β-amino ester)-functionalised magnetic nanoparticles for efficient gene delivery, Aust. J. Chem. 69 (2016) 349, https://doi.org/10.1071/CH15293.
[46] D.K. Owens, R.C. Wendt, Estimation of the surface free energy of polymers, J. Appl. Polym. Sci. 13 (1969) 1741–1747, https://doi.org/10.1002/app.1969.070130815.
[47] B.A. Trofimov, L.M. Sinegovskaya, N.K. Gusarova, Vibrations of the S–S bond in elemental sulfur and organic polysulfides: a structural guide, J. Sulfur Chem. 30 (2009) 518–554, https://doi.org/10.1080/17415990902998579.
[48] J. Xu, X. Rong, T. Chi, M. Wang, Y. Wang, D. Yang, F. Qiu, Preparation, characterization of UV-curable waterborne polyurethane-acrylate and the application in metal iron surface protection, J. Appl. Polym. Sci. 130 (2013) 3142–3152, https://doi.org/10.1002/app.39539.
[49] J. Zhou, H. Xu, L. Tang, Facile fabrication of high performance hydrophilic anti-icing polyurethane methacrylate coatings cured via UV irradiation, Prog. Org. Coat. 182 (2023), 107657, https://doi.org/10.1016/j.porgcoat.2023.107657.